Journal of Power Sources 273 (2015) 216–222

Contents lists available at ScienceDirect

Journal of Power Sources

journal homepage: www.elsevier.com/locate/jpowsour

An experimental study on burning behaviors of 18650 lithium ion batteries using a cone calorimeter

Yangyang Fu, Song Lu, Kaiyuan Li, Changchen Liu, Xudong Cheng, Heping Zhang*

State Key Laboratory of Fire Science, University of Science and Technology of China, Hefei, Anhui 230026, China

HIGHLIGHTS

- Fire risks and behaviors of charged lithium ion batteries were investigated.
- The thermal runaway of charged lithium ion batteries was experimentally studied.
- The effects of state of charge on burning behaviors of LIBs were evaluated.
- The heat release rates of LIBs were experimentally measured.
- The internal generated oxygen accounts for up to 13% of total heat release rate.

ARTICLE INFO

Article history:
Received 26 May 2014
Received in revised form
15 August 2014
Accepted 7 September 2014
Available online 16 September 2014

Keywords:
Lithium ion battery
Heat release rate
Thermal runaway
Thermal hazard
Explosion

ABSTRACT

Numerous of lithium ion battery fires and explosions enhance the need of precise risk assessments on batteries. In the current study, 18650 lithium ion batteries at different states of charge are tested using a cone calorimeter to study the burning behaviors under an incident heat flux of 50 kW m^{-2}. Several parameters are measured, including mass loss rate, time to ignition, time to explosion, heat release rate (HRR), the surface temperature and concentration of toxic gases. Although small quantities of oxygen are released from the lithium ion battery during burning, it is estimated that the energy, consuming oxygen released from the lithium ion battery, accounts for less than 13% of total energy released by a fully charged lithium ion battery. The experimental results show that the peak HRR and concentration of toxic gases rise with the increasing the states of charge, whereas the time to ignition and time to explosion decrease. The test results of the fully charged lithium ion batteries at three different incident heat fluxes show that the peak HRR increases from 6.2 to 9.1 kW and the maximum surface temperature increases from 662 to 934 °C as the incident heat flux increases from 30 to 60 kW m^{-2}.

© 2014 Elsevier B.V. All rights reserved.

1. Introduction

The lithium ion batteries (LIBs) have been widely used in electronic products, vehicles and aerospace applications owing to their excellent features of high power capacity, stable voltage, long life cycle and low self-discharge [1,2]. However, the LIBs fires and explosions have occurred occasionally in the transportation because their thermal stability is sensitive to temperature, overcharging, extrusion and collision. For instance, the Asiana Airlines' B747 freighter crashed into the sea on July 29, 2011, killing two pilots, due to a cargo fire caused by LIBs [3]. Therefore, to ensure the safety transportation of LIBs, it is worthwhile to study the burning behaviors of LIBs.

Previous researches have reported that the LIBs underwent thermal runaway reactions which lead to the combustion of organics electrolyte and rupture under heating conditions [4,5]. Jhu et al. [6] conducted a set of experiments in an adiabatic calorimeter and found that the charged LIBs were more hazardous than uncharged ones and the maximum surface temperature of the charged LIB could reach 903 °C. Roth et al. [7] showed that the thermal runaway reactions of LIBs were affected by the state of charge (SOC) using an accelerating rate calorimeter. Increasing SOC reduced the onset temperature of thermal runaway reactions and increased acceleration rate. Ribière et al. [8] demonstrated the fire-induced hazards of Li-ion polymer batteries using a Tewarson calorimeter. It was found that the HRR and toxic gases productions depended significantly on the SOC. Golubkov et al. [9] concluded that the maximum surface temperature of LIBs with the format 18650 was 850 °C as measured using a custom-designed test stand. The above researches have concentrated on the LIB burning

* Corresponding author. Tel.: +86 551 63600572 (office).
E-mail address: zhanghp@ustc.edu.cn (H. Zhang).

http://dx.doi.org/10.1016/j.jpowsour.2014.09.039
0378-7753/© 2014 Elsevier B.V. All rights reserved.

behaviors while heated using different calorimeters. However, cone calorimeter, as an important apparatus in hazardous material assessments, has not yet been applied to evaluate the burning behaviors of LIBs. Of the many fire reaction properties measured by the cone calorimeter, it is generally recognized that the HRR is the most important factor in controlling fire hazards, which corresponds directly to the intensity of fire. The HRR has been studied by Ribière using the Tewarson calorimeter. Their estimate of the maximum energy, liberated by the Joule effect which cannot indeed be related to O_2 consumption, is about 10% of the overall energy of a fully charged Li-ion polymer battery. The present work is to estimate the HRR of format 18650 LIB using the cone calorimeter. The HRR is estimated by oxygen depletion and mass loss methodologies, providing experimental data to infer the amount of released energy using up oxygen liberated from the LIB. Then this work investigates the burning behaviors of LIBs. The experiments focus on two aspects: (1) the effect of the SOC on the burning behaviors of LIBs, (2) the burning behaviors of the fully charged LIBs at different incident heat fluxes. The collected data by the cone calorimeter can be either used directly by researchers or used as input data for mathematical models to analyze the thermal and chemical threats [10].

2. Brief introduction to format 18650 lithium ion battery

An 18650 lithium ion battery mainly consists of a positive electrode (cathode), a negative electrode (anode), a separator and electrolyte. The cathode is a lithium cobalt oxide and the anode is graphite. Lithium ions are extracted from the anode and flow into the cathode during discharge. The ions reverse direction during charge [11].

As shown in Fig. 1, the LIB has a diameter of 18 mm and a length of 65 mm. The separator is a very thin sheet of micro-perforated plastic allowing ions to pass through, which is located between the cathode and anode separating the positive and negative electrodes. The electrolyte is a solution consisting of organic solvent and inorganic salt, which provides the media for lithium ions transport. The LIB is constructed by winding long strips of electrodes into a "jelly roll" configuration. Electrode stacks or rolls can be inserted into hard cases that are sealed with gaskets. The enclosure of a hard case cell is aluminum. A burst disk is used as safety vent [12].

3. Experimental setup

3.1. Samples

The LIBs used in the current study are manufactured by Sanyo. Table 1 shows the information of LIBs. The nominal capacity of the LIB is 2.6 Ah. The LIB is charged to the expected SOC and then put in the cone calorimeter to research the burning behaviors.

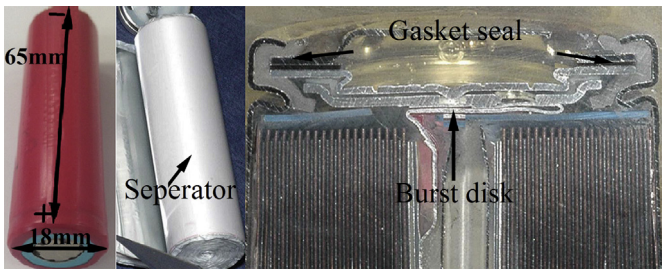

Fig. 1. Structure of the lithium ion battery.

Table 1
Information of commercial 18650 lithium-ion batteries.

Sample	Producer	Type	Capacity (Ah)	SOC (%)
A	Sanyo	UR18650FM	2.6	100
B	Sanyo	UR18650FM	2.6	70
C	Sanyo	UR18650FM	2.6	65
D	Sanyo	UR18650FM	2.6	50
E	Sanyo	UR18650FM	2.6	0

3.2. Apparatus

The cone calorimeter experiments were carried out according to the procedures in the ISO 5660-1 standard [13]. The samples were put horizontally in a sample holder staying on a load cell. Ceramic fiber blanket was used underneath the samples for thermal insulation. The sample holder was covered by a wire grid to prevent the LIB explosion splashing sparks from attaching the cone heater during the test. Two K-type thermocouples were wound around the sample using steel wires, which attaching the sample surface at different locations in order to obtain the surface temperature. The cone calorimeter was calibrated according to the procedure in the ISO 5660-1 standard before experiments. Protection screen was put down to prevent explosion splashing sparks from widely spreading. Fig. 2 presents the experimental setup in the cone calorimeter. As shown in Fig. 2, the surface of the sample was radiated by the cone heater and heated up. The combustion productions were collected by an exhaust hood and transported away through a ventilation system. CO and CO_2 gas analyzers were used to measure the generation of carbon monoxide and carbon dioxide. An O_2 analyzer was used to measure the oxygen depletion. The fan flow rate was set as 24 L s^{-1}. A camera was positioned to observe the burning process of the LIB. The ambient temperature was around 30 °C with natural ventilation. The experiments ended when flame was extinguished. Each experiment was repeated at least three times and the average values were taken.

During the test, the following parameters were determined: mass loss rate, the time to ignition and the time to explosion, the yields of CO and CO_2, the surface temperature and HRR. The sample was weighted using a load cell. The time to ignition is defined as the duration time which is needed by the sample from being exposed to incident radiation till a visible and sustainable flame is firstly established. The time to explosion is time from experiment start to explosion. The observation of time to ignition and explosion were recorded. The temperature readings were recorded using the Agilent 34970A data acquisition system. The HRR and the yields of CO and CO_2 were recorded automatically by the cone calorimeter.

4. Results and discussion

4.1. Burning process

The experimental process shows the LIB reacts strongly while being heated. Fig. 3 presents the typical burning process of a fully

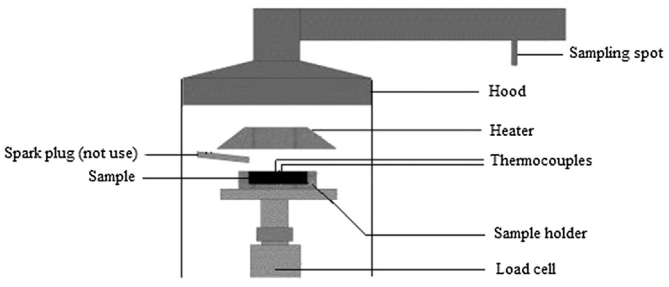

Fig. 2. Experimental setup in the cone calorimeter.

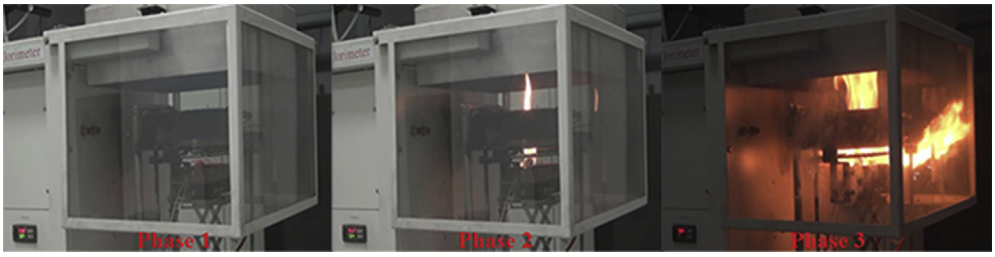

Fig. 3. Burning process of the fully charged LIB obtained in the experiment.

charged LIB during the experiment. The sample undergoes 3 noticeable stages during the experiment. At the stage 1, the sample mainly experiences a smoldering stage with no flame presented while in phase 2 a sustainable flame is observed above the sample. Stage 2 would last for several tens of seconds before the burning process goes into stage 3 in which a severe explosion takes place. When the sample is exposed to heat flux, the surface temperature of the sample gradually increases. The temperature curve versus time is plotted in Fig. 4, where the surface temperature is the average value obtained from the two thermocouples attached at the exposed sample surface. The increasing surface temperature makes the package plastic to melt and the generation of gas in the LIB results in the swelling of the LIB. Soon after, it is seen that the burst disk cracks and small amount of gas releases. At the same time, the surface temperature increases significantly at 125 °C because of solid electrolyte interface (SEI) layer breaking down exothermically. Consequently the intercalated lithium directly reacts with the organic electrolyte and generates more heat [14,15]. Due to the new SEI layer preventing the electrolyte from continuously reacting with intercalated lithium, there is a minor temperature decrease at approximately 255 °C. The new SEI layer is formed by intercalated lithium reacting with the electrolyte [15]. Then the surface temperature further rises because the new SEI layer decomposes exothermically with the increasing temperature. When the temperature is over 264 °C, the surface temperature increases sharply from 264 °C to the maximum temperature of 747 °C within 10 s, which is a result of the thermal runaway reactions. It is also observed that a violent explosion occurs with the cap assemblies of the LIB ejected and a large amount of gas released, and then the fragments and evolved gases are ignited. When the explosion ends, the temperature decreases slowly, as shown in Fig. 4.

The temperature increasing rate against the surface temperature is plotted in Fig. 5. In the experiment, the cone heater heats up the sample surface and raises the surface temperature from 30 to 125 °C. Then the sample starts to react exothermically and reaches the first peak of increasing rate at 148 °C. However, a sudden decline is caused by the endothermic separator fusing [7], as shown in Fig. 5. It is noted that the temperature increasing rate starts to arise distinctly at the temperature around 264 °C which is regarded as the onset temperature of thermal runaway reactions, at which a sufficient concentration of flammable vapor is produced.

By reference to Roth et al. [16], the SEI layer decomposes at 90–130 °C, intercalated lithium reacts with the electrolyte at 90–290 °C (electrolyte decomposes at 200–300 °C), and positively active materials decompose and react with the solvent at 150–500 °C. The endothermic reactions start about 170 °C, followed by exothermic reactions in the temperature range of 170–330 °C according to the ARC tests [17]. The results of the cone calorimeter experiments are basically consistent with those obtained by other calorimetric methodologies.

4.2. Time to ignition and time to explosion

The time to ignition and time to explosion of LIBs are listed in Table 2. It can be seen that the time to ignition significantly changes with the SOCs under the same incident heat flux. The higher the SOC is, the shorter time to ignition is. However, the LIBs with 0 and 50% SOC are shorter than that of the LIB with 65% SOC. The time to

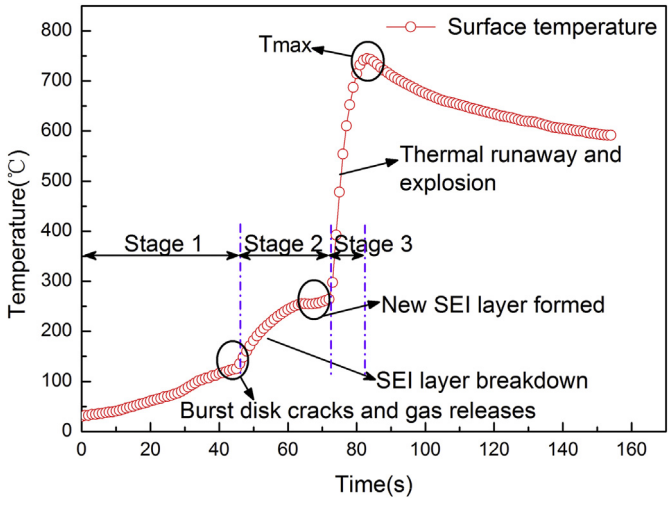

Fig. 4. Temperature profile with time of the fully charged LIB under an incident heat flux of 50 kW m^{-2}.

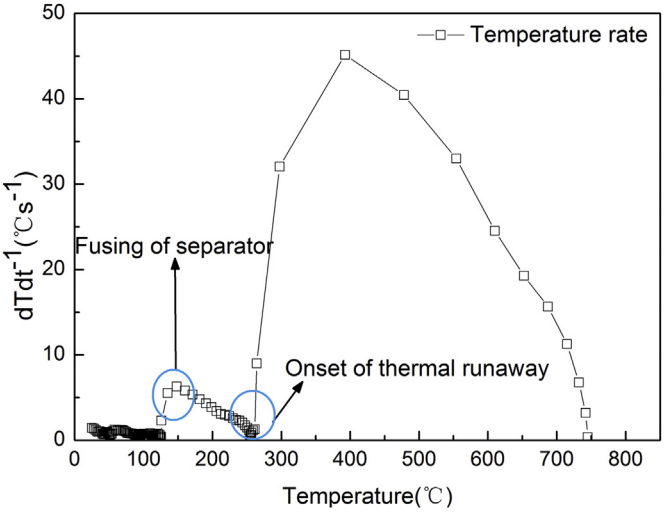

Fig. 5. The temperature rate versus the temperature of the fully charged LIB under an incident heat flux of 50 kW m^{-2}.

Table 2
Time to ignition and time to explosion of LIBs.

Incident heat flux (kW m^{-2})	SOC (%)	Time to ignition (s)	Time to explosion (s)
50	100	40	81
50	70	83	156
50	65	131	200
50	50	49	Not explode
50	0	72	Not explode
30	100	157	182
60	100	17	55

ignition of the fully charged LIB is the shortest of the LIBs at different SOCs, indicating that the fully charged LIB ignites more easily and shows high fire risk. It also can be observed that the ignition time is inverse function of the incident heat flux. The higher the incident heat flux is, the shorter is the ignition time. In theory, the temperature and concentration of combustible gas are directly relevant to ignition. Fig. 6 presents the surface temperatures measured in the experiments. From Fig. 6, the surface temperature increases as the incident heat flux increases. For high incident heat fluxes, the surface temperature increases speedy, the thermal decomposition of the LIB is also rapid and produces a large amount of gas. As a result, the time to ignition is short. On the other hand, for low incident heat fluxes, the surface temperature increases slowly, the emission of gas is slow so that the time to ignition is relatively long.

The time to explosion decreases with the increasing SOCs. Table 2 presents the fully charged LIB explodes at 81 s while the LIB with 65% SOC explodes at 200 s. However, the LIBs with the 50 and 0% SOC do not explode during the experiments.

4.3. Heat release rate

As the HRR is the most critical factor which governs thermal hazards in a given scenario and determines whether a neighbor LIB will be ignited in a battery pack [18], it needs to be seriously considered when assessing the fire risks of battery pack. There are a series of methodologies developed to evaluate the HRR, such as methodologies of oxygen depletion, mass loss [19,20] and temperature rise [21]. The oxygen depletion based on Thornton's principle [22] is the most frequently used methodology. For a large number of organic solids or liquids or gaseous, Thornton found that the amount of energy released by a complete burning material was proportional to the amount of O_2 consumed by the combustion reactions. The advantage of this methodology is the direct use of oxygen mass without the knowledge of the material chemical composition or the combustion chemistry. The HRR can be determined using Equation (1).

$$\dot{q} = E\left(\dot{m}^0_{O_2} - \dot{m}_{O_2}\right) \tag{1}$$

where $\dot{q}$ is the heat release rate (kW), $\dot{m}^0_{O_2}$ and $\dot{m}_{O_2}$ are the mass flow rates of oxygen from the incoming air and in the exhaust duct, respectively (kg s^{-1}). $E = 13.1 \pm 5\%$ MJ kg^{-1} is the energy released per mass unit of O_2 consumed for a given fuel [23]. In this work, the HRR is measured by oxygen depletion method and calculated by mass loss method.

Fig. 7 shows the HRRs estimated using the two methods. The mass loss rate is recorded by the load cell and the heat of combustion of a fully charged LIB is found in the literature [12]. The HRR is calculated using the Equation (2) [18],

$$\dot{q} = \chi \Delta H_c \dot{m}_{\text{fuel}} \tag{2}$$

where $\dot{m}_{\text{fuel}}$ is the mass loss rate (kg s^{-1}), $\Delta H_c = 6.2$ MJ kg^{-1} is the heat of combustion, and χ denotes the combustion efficiency ($\chi = 0.78$) [18].

From Fig. 7, the HRR curves can be also divided into 3 stages. At the stages 1 and 2, the HRR values are relatively low, while the ones at the stage 3 are extremely high representing the LIB explosion happening. A comparison between the two methods indicates that the HRR curves are substantially identical. As shown in Fig. 7, the HRR curves of the two methods almost overlap as zero at the stage 1 due to the absence of flame. However, the HRR values estimated by oxygen depletion method are lower than that calculated values using Equation (2) at the stages 2 and 3. This can be attributed to that the oxygen depletion method underestimates the actual oxygen consumed as the chemical reactions inside the LIB can produce a spot of oxygen during the burning.

The calculated HRR values using Equation (2) increase slightly beyond 40 s. However, at approximately 77 s, the calculated HRR curve presents a steep decrease, which is caused by the pressure generated by the explosion. The load cell is pressed suddenly and

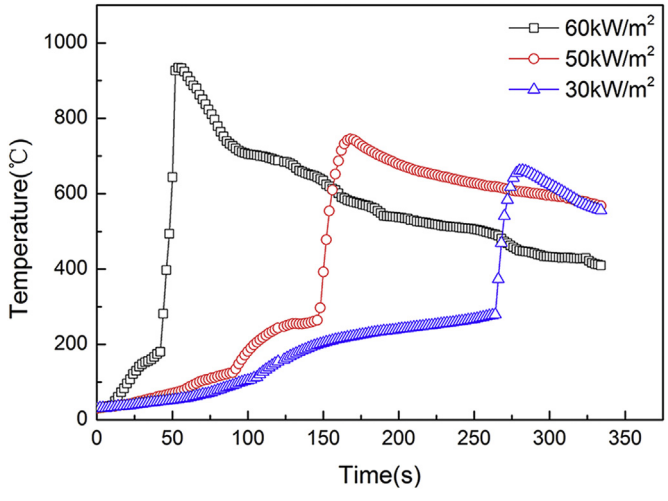

Fig. 6. Temperature profiles of the fully charged LIBs under incident heat fluxes of 30, 50 and 60 kW m^{-2}.

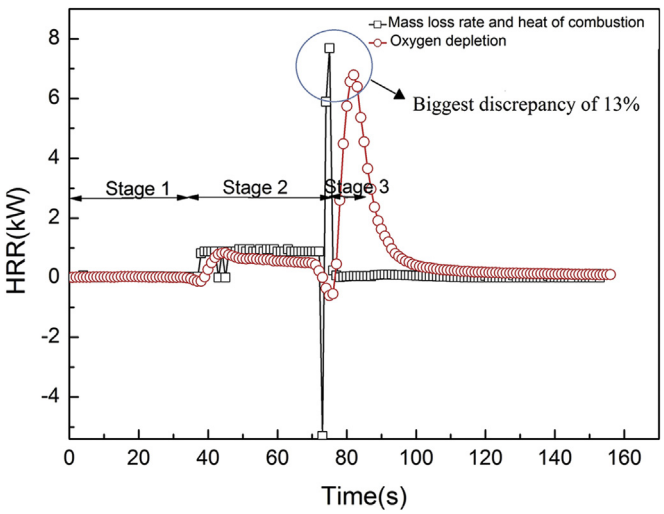

Fig. 7. HRR profiles of the fully charged LIB under an incident heat flux of 50 kW m^{-2}.

results in a sharp increase of mass reading. Shortly afterward, the calculated HRR value increases again and reaches the peak HRR.

At the stage 2, the positive HRR values obtained by oxygen depletion method correspond to the packaged plastic melting and gas burning while the negative HRR values at about 44 s and 75 s are caused by the oxygen released from the decompositions of cathode and anode, as observed in Fig. 6. Kumari et al. [24] claims that generation of O_2 is due to the decomposition of cathode. MacNeil et al. [25,26] reports that above 200 °C the delithiated $Li_{0.5}CoO_2$ decompose and release O_2 as:

$$Li_{0.5}CoO_2 \rightarrow \frac{1}{2}LiCoO_2 + \frac{1}{6}Co_3O_4 + \frac{1}{6}O_2 \quad (3)$$

Co_3O_4 can decompose with the presence of solvent at 400 °C and release O_2 and CoO. The CoO can further decompose at 473 °C and release O_2.

$$Co_3O_4 \rightarrow 3CoO + \frac{1}{2}O_2 \quad (4)$$

$$CoO \rightarrow Co + \frac{1}{2}O_2 \quad (5)$$

In the meantime, the negative electrode also releases O_2.

$$(CH_2OCO_2Li)_2 \rightarrow Li_2CO_3 + C_2H_4 + CO_2 + \frac{1}{2}O_2 \quad (6)$$

At the stage 3, the HRR values obtained by oxygen depletion method correspond to the thermal runaway reactions and explosion. The energy is fleetly released and the peak HRR swiftly reaches, which might be explained by the presence of acidic C–H bonds of imidazolium cations easily converted into NHC-carbenes under heat conditions [27].

It should be noted that although small quantities of oxygen are released from the energetic LIB during the burning, the internally generated oxygen has insignificant effect on the combustion process and the HRR. The comparison between the measured and calculated HRR values shows the biggest discrepancy is approximately 13%, as shown in Fig. 7. Therefore, it is estimated that the energy, consuming the O_2 released by the internal redox reactions, accounts for less than 13% of the overall energy released by a fully charged LIB. This confirms the feasibility of using cone calorimeter for the HRR determination.

4.3.1. Effect of the state of charge on heat release rate

The SOC of the LIB is one of the most critical factors to the chemical reactions and it should be less than 50% to minimize degradation and aging during the transportation [28]. Fig. 8 shows the HRR profiles of LIBs with the SOCs from 0 to 100% under an incident heat flux of 50 kW m^{-2}. The HRR profiles of LIBs with 50 and 0% SOC exhibit similarly while the others are closely resemble. As shown in Fig. 8, the SOC has an effect on both the time to the peak HRR and the magnitude of the peak HRR. The peak HRR values reach 6.8, 6.5, 5.8, 1.5 and 1.1 kW for 100, 70, 65, 50 and 0% SOC, respectively. It can be concluded that the fully charged LIB is more risky compared to the others as it produces the highest HRR, whereas the LIB with 0% SOC is the safest case with the lowest HRR and without explosion. This is probably because that the HRR is affected by the stored electrical energy which is stored as potential chemical energy [29]. The more energy a LIB has stored, the more energetic the exothermic reactions of the electrodes with the electrolytes will be, the more heat and gas generated will be, the easier the explosion occurs. Thus, it can be concluded that the burning hazards of the LIB rises with the increasing SOCs and less than 50% SOC is reasonable to be suggested in the transportation.

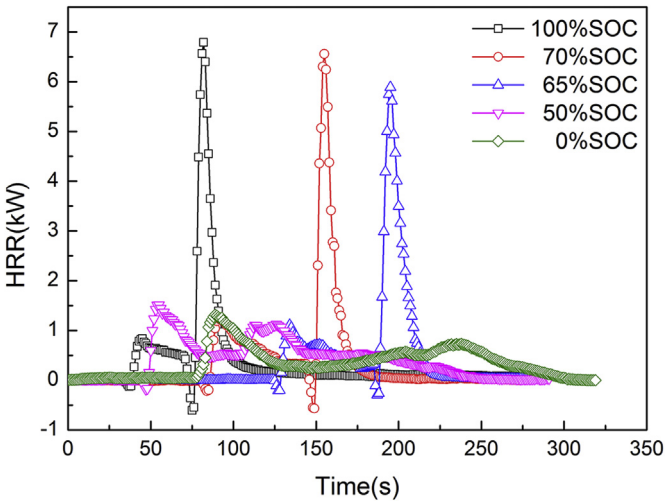

Fig. 8. HRR profiles of LIBs at different states of charge under an incident heat flux of 50 kW m^{-2}.

Integrating the HRR curves gives the total energy released during the burning which ends up as approximately 100, 101, 104, 120 and 109 kJ for 100, 70, 65, 50 and 0% SOC, respectively. It is noted that the fully charged LIB releases the least energy but has the highest HRR value. This might be attributed to two aspects: (1) the explosion suddenness restricts the oxygen consumption, leading to incomplete combustion [8], (2) the internal released oxygen is involved in the combustion in relatively short burning process.

4.3.2. Effect of incident heat flux on heat release rate

Fig. 9 shows the HRR profiles of LIBs with 100% SOC under incident heat fluxes of 30, 50 and 60 kW m^{-2}. It is found that the LIBs burn much more vigorously under high incident heat fluxes of 50 and 60 kW m^{-2} than that under 30 kW m^{-2}. The increasing incident heat fluxes have a strong influence on the intensities of thermal degradation and thermal runaway reactions. It can be seen in Fig. 9 that the peak HRR values increase with the increasing incident heat fluxes. According to the experimental results, the peak HRR increase from 6.2 to 9.1 kW as the incident heat flux increase from 30 to 60 kW m^{-2}.

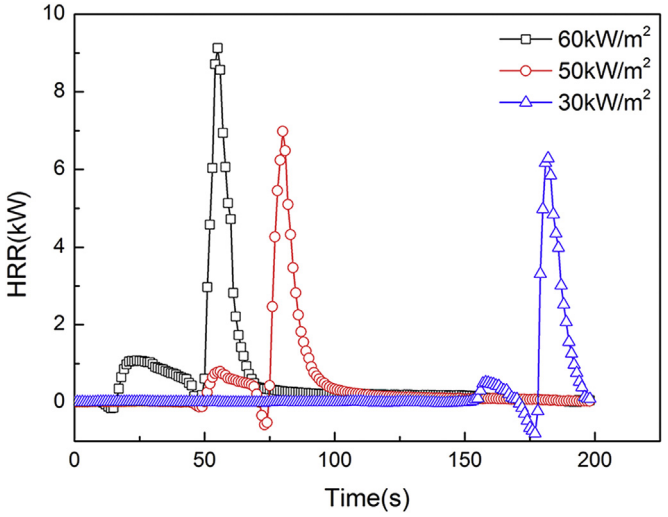

Fig. 9. HRR profiles of the fully charged LIBs under incident heat fluxes of 30, 50 and 60 kW m^{-2}.

4.4. Gas analysis

Another key factor related to fire is the toxic gases released. Figs. 10 and 11 show the CO_2 and CO productions profiles for different experimental conditions. From Figs. 10 and 11, CO and CO_2 productions increase with the increasing SOCs. O_2 is generated from the decomposition of the overcharged delithiated $LiCoO_2$ as in Equation (3). The air inside the LIB contains CO_2 and the redox reactions in the LIB also generate CO_2 as in Equations (7)–(9). The oxidation reactions of electrolyte and O_2 in the LIB release CO_2 [30]:

$$C_3H_6O_3 + 3O_2 \rightarrow 3CO_2 + 3H_2O \quad (7)$$

The other reactions of water and HF (decomposition product of LiPF6) in the electrolyte are:

$$LiOCO_2CH_3 + HF \rightarrow LiF + CH_3OH + CO_2 \quad (8)$$

$$(CH_2OCO_2Li)_2 + H_2O \rightarrow Li_2CO_3 + 2CH_2OH + CO_2 \quad (9)$$

The carbon monoxide is likely to be generated from the reduction of CO_2 with intercalated Li at the anode.

$$2CO_2 + 2Li^+ + 2e^- \rightarrow Li_2CO_3 + CO \quad (10)$$

Another source of the carbon monoxide may be the incomplete combustion.

As a result, higher SOCs will lead to larger amount of O_2. The increasing concentration of oxygen will lead to more CO_2 and CO productions according to Equations (7) and (10) consequently.

At the ignition point both the CO and CO_2 emitted from the LIB increase because the CO and CO_2 increase when the flame appears. The CO and CO_2 generation rates present a significant increase at which the LIB goes into thermal runaway reactions till explosion and then decrease rapidly.

5. Conclusions

This study has examined the burning behaviors of LIBs using the cone calorimeter with key parameters including the HRR, mass loss rate, the time to ignition and concentration of toxic gases investigated. The HRR was analyzed using oxygen depletion and mass loss methodologies. From the comparison of the two methods, it is concluded that the energy, consuming oxygen released from the LIB, accounts for less than 13% of the overall energy released by a fully charged LIB. The LIBs with 100, 70, 65, 50 and 0% SOC were evaluated under incident heat flux of 50 kW m^{-2} while the LIBs with 100% SOC were tested under different incident heat fluxes of 30, 50 and 60 kW m^{-2}. The results show that the SOC has significant effects on the burning behaviors as the stored electrical energy plays an important role in burning process. According to result, the fully charged LIB presents the highest surface temperature of 797 °C, the maximum peak HRR value of 6.8 kW, the shortest time to ignition of 40 s, the shortest time to explosion of 81 s and the highest CO and CO_2 productions of respective 38 kg kg^{-1} and 348 kg kg^{-1}. As a result, the fully charged LIBs are more dangerous than the others.

With respect to the effect of incident heat flux, exposing the LIBs to high incident heat fluxes would be very dangerous, as the accumulation of heat at the surface might cause severe thermal decomposition and thermal runaway reactions. The temperature control of the LIB is crucial to prevent the occurrence of thermal runaway reactions. The surface temperature and the peak HRR increase as the incident heat flux increases while the time to ignition and time to explosion decrease. The highest temperature reaches 934 °C at 60 kW m^{-2} which is far more than the ignition temperature of normal combustible materials. The burning LIB could ignite adjacent batteries in the battery pack and cause the entire batteries to ignite or rupture. The current results also indicate that applying the cone calorimeter to evaluate the thermal hazards of LIB is a reasonable technique in LIB safety assessments. Future work will focus on the thermal behaviors of multiple LIBs in a module triggered by heating conditions.

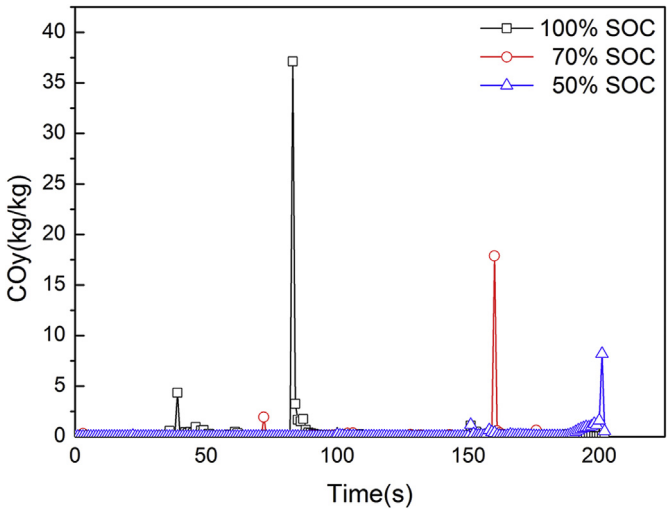

Fig. 10. CO production profiles of LIBs at different states of charge under an incident heat flux of 50 kW m^{-2}.

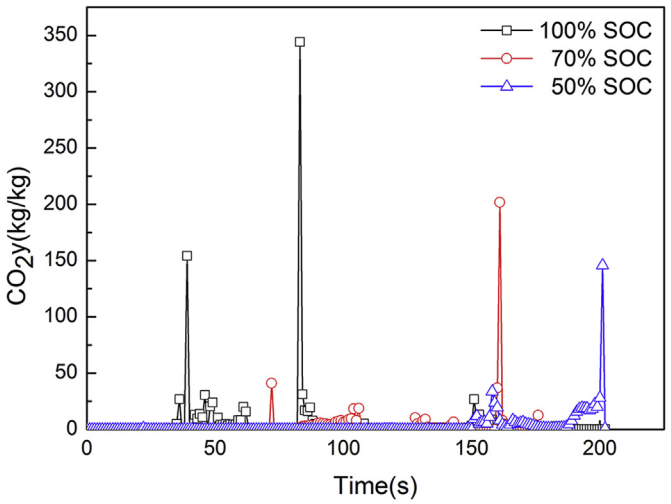

Fig. 11. CO_2 production profiles of LIBs at different states of charge under an incident heat flux of 50 kW m^{-2}

Acknowledgements

This study was supported by the National Natural Science Foundation of China (No. 71403254) and the China Postdoctoral Science Foundation (No. 2014M551823).

References

[1] T.M. Bandhauer, S. Garimella, T.F. Fuller, J. Electrochem. Soc. 158 (2011) R1–R25.
[2] H.J. Noh, S. Youn, C.S. Yoon, Y.K. Sun, J. Power Sources 233 (2013) 121–130.
[3] AirportWatch, Air Freight News, 2011. http://www.airportwatch.org.uk/?p=3521.

[4] C. Arbizzani, G. Gabrielli, M. Mastragostino, J. Power Sources 196 (2011) 4801–4805.
[5] C.Y. Jhu, Y.W. Wang, C.Y. Wen, C.C. Chiang, J. Therm. Anal. Calorim. 106 (2011) 159–163.
[6] C.Y. Jhu, Y.W. Wang, C.M. Shu, J.C. Chang, H.C. Wu, J. Hazard. Mater. 192 (2011) 99–107.
[7] E.P. Roth, D.H. Doughty, J. Power Sources 128 (2004) 308–318.
[8] P. Ribière, S. Grugeon, M. Morcrette, S. Boyanov, S. Laruelle, Energy Environ. Sci. 5 (2012) 5271.
[9] A.W. Golubkov, D. Fuchs, J. Wagner, H. Wiltsche, C. Stangl, G. Fauler, G. Voitic, A. Thaler, V. Hacker, RSC Adv. 4 (2014) 3633.
[10] K.C. Tsai, J. Hazard. Mater. 172 (2009) 763–772.
[11] Q. Wang, P. Ping, X. Zhao, G. Chu, J. Sun, C. Chen, J. Power Sources 208 (2012) 210–224.
[12] M. Celina, K. Michael, W. Kevin, T.L. Richard, Fire Protection Research Foundation, 2011.
[13] ISO 5660-1, Reaction to Fire Tests – Heat Release Smoke Production and Mass Loss Rate Part1 Heat Release Rate, 2002.
[14] T. Ohsaki, T. Kishi, T. Kuboki, N. Takami, N. Shimura, Y. Sato, M. Sekino, A. Satoh, J. Power Sources 146 (2005) 97–100.
[15] Q. Wang, J. Sun, X. Yao, C. Chen, J. Electrochem. Soc. 153 (2006) A329.
[16] E.P. Roth, D.H. Doughty, J. Franklin, J. Power Sources 134 (2004) 222–234.
[17] J.S. Gnanaraj, E. Zinigrad, L. Asraf, H.E. Gottlieb, M. Sprecher, D. Aurbach, M. Schmidt, J. Power Sources 119–121 (2003) 794–798.
[18] G.G. Eshetu, S. Grugeon, S. Laruelle, S. Boyanov, A. Lecocq, J.P. Bertrand, G. Marlair, Phys. Chem. Chem. Phys. : PCCP 15 (2013) 9145–9155.
[19] ISO 5660, Fire Tests–reaction to Fire–part 1: Rate of Heat Release from Building Products (Cone Calorimeter), ISO, Geneva, 1993.
[20] ASTM 1354–905, Standard Test Method for Heat and Visible Smoke Release Rates for Materials and Products Using an Oxygen Consumption Calorimeter, ASTM, Philadelphia, 1995.
[21] ASTM E-906, Standard Test Method for Heat and Visible Smoke Release Rates for Materials and Products, ASTM, Philadelphia, 1983.
[22] W.M. Thornton, Philos. Mag. Ser. 633 (1917) 196–203.
[23] C. Huggett, Fire Mater. 4 (2) (1980) 61–65.
[24] K. Kumai, H. Miyashiro, Y. Kobayashi, K. Takei, R. Ishikawa, J. Power Sources 81 (1999) 715.
[25] D.D. MacNeil, J.R. Dahn, J. Electrochem. Soc. 149 (2002) A912–A919.
[26] D.D. MacNeil, J.R. Dahn, J. Electrochem. Soc. 148 (2001) A1205–A1210.
[27] H. Yao, J. Zhang, Y. Zhang, H. Sun, Q. Shen, Organometallics 29 (2010) 5841–5846.
[28] D. Michael, J. Power Sources 96 (2001) 260–265.
[29] K. White, Q. Horn, S. Singh, R. Spray, N. Budiansky, in: Proceedings, 28th International Battery Seminar and Exhibit, Ft. Lauderdale, FL, 2011, pp. 14–17.
[30] K. Kazuma, M. Hajime, J. Power Sources 81–82 (1999) 715–719.